

The Galactic positron flux and dark matter substructures

Qiang Yuan and Xiao-Jun Bi

Key Laboratory of Particle Astrophysics, Institute of High Energy Physics, Chinese Academy of Sciences, P.O.Box 918-3, Beijing 100049, P. R. China

E-mail: yuanq@ihep.ac.cn, bixj@ihep.ac.cn

Abstract. In this paper we calculate the Galactic positron flux from dark matter annihilation in the frame of supersymmetry, taking the enhancement of the flux by existence of dark matter substructures into account. The propagation of positrons in the Galactic magnetic field is solved in a realistic numerical model GALPROP. The secondary positron flux is recalculated in the GLAPROP model. The total positron flux from secondary products and dark matter annihilation can fit the HEAT data well when taking a cuspy density profile of the substructures.

PACS numbers: 95.35.+d

Keywords: dark matter, positron, propagation

1. Introduction

The astronomical observations indicate that most of the matter in our universe is dark (see for example [1]) for a long time. The evidences come mainly from the gravitational effects of the dark matter component, such as the rotation curves of spiral galaxies [2], the gravitational lensing [3] and the dynamics of galaxy clusters [4]. The studies of primordial nucleosynthesis [5], structure formation [6] and cosmic microwave background (CMB) [7] show that this so-called dark matter (DM) is mostly non-baryonic. The nature of the non-baryonic dark matter remains one of the most outstanding puzzles in particle physics and cosmology.

A large amount of theoretical models of DM have been proposed in literatures [8]. All these candidates of non-baryonic DM particles require physics beyond the standard model of particle physics. Among the large amount of candidates, the most attractive scenario involves the weakly interacting massive particles (WIMPs). In particular, the minimal supersymmetric extension of the standard model (MSSM) provides an excellent WIMP candidate as the lightest supersymmetric particle (LSP), usually the neutralino, which are stable due to R-parity conservation [1].

WIMPs are possible to be detected beyond the gravitational effects. One viable way is to detect the elastic scattering signals of DM particles on the detector nuclei (direct searches) [9, 10, 11, 12]. This is the most sensitive method at present for DM detection

[13]. Another way is to search the self-annihilation products of the DM particles (indirect searches), such as neutrinos [14], γ -rays [15, 16], antiprotons [17] and positrons [18, 19]. Since the positrons, antiprotons and diffuse γ -rays are secondary particles in the cosmic rays with low fluxes, these kinds of dark matter annihilation (DMA) products are easier to be distinguished from the astrophysical background. Direct and indirect detections of DM particles are complementary ways to each other.

The balloon-borne instrument High-Energy Antimatter Telescope (HEAT) was designed to determine the positron fraction over a wide energy range with high statistical and systematic accuracy. Based on the three flights(1994, 1995 and 2000), this collaboration reported an excess of positrons with energies higher than several GeV and peaked in the range $7 \sim 10 \, GeV$ [20, 21]. It seems that the astrophysical production cannot give enough positrons as observed [22], and there might exist exotic sources of positrons. It has been pointed out that the excess may indicate the signal of DM annihilation [18, 19]. However, Baltz *et al* showed that for supersymmetry (SUSY) DM a “boost factor” ≥ 30 has to be introduced to fit the HEAT data [23]. It was thought that the local clumpiness of DM distribution might account for this “boost factor”. However, Hooper *et al* argued that it was less possible for a DM clump to be close enough to the Earth to contribute sufficient positron flux [24].

Stimulated by the recent numerical simulation which shows that the lightest subhalos in the Galaxy could be extended to $10^{-6} M_{\odot}$ with a huge amount of about 10^{15} [25], we try to calculate the Galactic positron flux again in the frame of supersymmetry taking the enhancement by the large amount of subhalos into account. There was effort try to explain the HEAT data by the nearby mini-clumps [26]. However, the possibility of this scenario is also extremely low [27]. Another difference of this work from the previous studies most of which adopt the Green’s function method to calculate the positron’s propagation is that we calculate its propagation in the Galactic magnetic field using the numerical package GALPROP [28], which adopts realistic distribution of interstellar gas and radiation field. Our result shows that the two methods lead to large difference. To give a consistent result we also calculate the secondary positron flux using GALPROP. The propagation parameters are adjusted to fit observations such as B/C, proton and electron spectra. Our results show that the secondary positron has better agreement with the HEAT data than these adopted in previous studies [18, 19, 23, 26] and decreases the tension between predictions and data.

The paper is organized as following: in Sec. 2 we present the SUSY model. In Sec. 3 we give our treatment of subhalos distribution and density profiles. Sec. 4 introduces the positron’s propagation and the GALPROP model. The results are given in Sec. 5.

2. Positron Production from Neutralino Annihilation

The LSP, generally the lightest neutralino, is stable in the R-parity conservative MSSM and provides a natural candidate of dark matter. It is a combination state of the supersymmetric partners of the photon, Z^0 boson and neutral Higgs bosons.

Positrons can be produced in several neutralino annihilation modes. Most of them come from the decay of gauge bosons produced in channels $\chi\chi \rightarrow ZZ$, $\chi\chi \rightarrow W^+W^-$, or from the cascades of final particles, such as fermions and Higgs bosons. The spectrum of positrons depends on the neutralino mass and its annihilation modes. There is also a direct channel $\chi\chi \rightarrow e^+e^-$ and produces monochrome positrons with energy $E_{e^+} = m_\chi$. However, the branching ratio of this channel is usually small. In the following discussion we neglect this “line” contribution to the positron spectrum.

The source function of positrons from DM annihilation can be written as

$$Q(E_{e^+}, \mathbf{r}) = \frac{\langle\sigma v\rangle}{2m_\chi^2} \frac{dn}{dE} \rho^2(\mathbf{r}), \quad (1)$$

where σ is the positron generating cross-section, dn/dE is the positrons spectrum in one annihilation by a pair of neutralinos and $\rho(\mathbf{r})$ is neutralino density distribution in space. The source term $Q(E_{e^+}, \mathbf{r})$ is given in unit of $GeV^{-1}cm^{-3}s^{-1}$.

The source term is calculated in MSSM by doing a random scan using the software package DarkSUSY [29]. In these SUSY models we choose a few models which satisfy all the experimental bounds and give large fluxes and appropriate spectrum so that we can fit the HEAT data well. However, there are more than one hundred free SUSY breaking parameters even for the R-parity conservative MSSM. A general practice is to assume some relations between the parameters and greatly reduce the number of free parameters. For the processes related with dark matter production and annihilation, only seven parameters are relevant under some simplifying assumptions, i.e., the higgsino mass parameter μ , the wino mass parameter M_2 , the mass of the CP-odd Higgs boson m_A , the ratio of the Higgs Vacuum expectation values $\tan\beta$, the scalar fermion mass parameter $m_{\tilde{f}}$, the trilinear soft breaking parameter A_t and A_b . To determine the low energy spectrum of the SUSY particles and coupling vertices, the following assumptions have been made: all the sfermions have common soft-breaking mass parameters $m_{\tilde{f}}$; all trilinear parameters are zero except those of the third family; the bino, wino, and gluino have the mass relations, $M_1 = 5/3 \tan^2 \theta_W M_2$, $M_3 = \alpha_3(M_Z)/\alpha_2(M_Z)M_2$, coming from the unification of the gaugino mass at the grand unification scale.

The parameters are constrained in the following ranges: $50GeV < |\mu|$, M_2 , M_A , $m_{\tilde{f}} < 10TeV$; $1.1 < \tan\beta < 55$; $-3m_{\tilde{q}} < A_t$, $A_b < 3m_{\tilde{q}}$; $\text{sign}(\mu) = \pm 1$. The SUSY models are required to satisfy the theoretical consistency requirement, such as the correct vacuum breaking pattern, the neutralino being the LSP and so on. The accelerator data constrains the models further from the spectrum requirement, the invisible Z-boson width, the branching ratio of $b \rightarrow s\gamma$ and the muon magnetic moment.

The constraint from cosmology is also taken into account by requiring the relic abundance of neutralino $0.091 < \Omega_\chi h^2 < 0.118$, which corresponds to the 3σ bound from the cosmological observations [7]. The effect of coannihilation between the fermions is taken into account when calculating the relic density numerically.

3. Dark Matter Distribution

To determine the positron source term from DM annihilation in Eq. (1) we have to specify the DM density profile $\rho(\mathbf{r})$. Based on the N-body simulation results the DM density profile can be written in a general form as [30]

$$\rho = \frac{\rho_s}{(r/r_s)^\gamma [1 + (r/r_s)^\alpha]^{(\beta-\gamma)/\alpha}}, \quad (2)$$

where ρ_s and r_s are the scale density and scale radius respectively. These two parameters are determined by the measurement of the virial mass of the halo and the concentration parameter determined by simulation. The NFW profile was first proposed by Navarro, Frenk and White [31] with $(\alpha, \beta, \gamma) = (1, 3, 1)$. However, Moore *et al.* gave another form of DM profile with $(\alpha, \beta, \gamma) = (1.5, 3, 1.5)$ to fit their simulation result [32]. The Moore profile has steeper slope near the Galactic center than the NFW profile. There are also simulations showing that the density profile may not be universal [33, 34]. Reed *et al.* show that $\gamma = 1.4 - 0.08 \log(M/M_*)$ increases for smaller subhalos [34]. Therefore we also adopt a $\gamma = 1.7$ profile for the whole range of subhalos from $\sim 10^{-6} M_\odot$ to $\sim 10^{10} M_\odot$ for simplicity. At present there are still controversial on which one represents the actual density profile.

To determine the parameters in the density profile, we adopt a semi-analytic model of Bullock *et al* [35], which describes the concentration parameter c_V as a function of viral mass and redshift. We adopt the mean $c_V - m_{\text{sub}}$ relation at redshift zero. The scale radius is then determined as $r_s^{\text{NFW}} = r_V/c_V$, $r_s^{\text{moore}} = r_s^{\text{NFW}}/0.63$ and $r_s^\gamma = r_s^{\text{NFW}}/(2-\gamma)$.

High resolution simulations have revealed that a large number of self-bound substructures survived in the galactic halos [36, 37, 38, 39, 40, 41, 42, 43]. Especially a recent simulation conducted by Diemand *et al.* [25] showed that the first generation objects as light as the Earth mass can survive until today. The number of such minihalos is huge, reaching 10^{15} . The existence of a wealth of subhalos will greatly enhance the DM annihilation flux, since the annihilation rate is proportional to the density square as shown in Eq. (1).

The simulations show that the number density of subhalos can be approximately given by an isothermal profile with a core [44]

$$n(r) = 2n_H(1 + (r/r_H)^2)^{-1}, \quad (3)$$

with r_H being about 0.14 times the halo virial radius $r_H = 0.14r_{\text{vir}}$. The result given above agrees well with that in another recent simulation by Gao *et al.* [45]. Eq. (3) shows that the radial distribution of substructures is generally shallower than the density profile of the smooth background in Eq. (2). This is due to the tidal disruption of substructures which is most effective near the galactic center.

The mass function is well fitted to the simulation result as $dn/dm_{\text{sub}} \propto m_{\text{sub}}^{-1.9}$. We then get the number density of substructures with mass m_{sub} at the position r to the galactic center

$$n(m_{\text{sub}}, r) = n_0 \left(\frac{m_{\text{sub}}}{M_{\text{vir}}} \right)^{-1.9} (1 + (r/r_H)^2)^{-1}, \quad (4)$$

where M_{vir} is the virial mass of the Milky Way (MW), n_0 is the normalization factor determined by requiring the number of subhalos with mass larger than $10^8 M_{\odot}$ is about 500 in a halo with $M = 2 \times 10^{12} M_{\odot}$ [38].

Taking the subhalos into account the density square in Eq. (1) is given by

$$\rho^2(\mathbf{r}) \rightarrow \langle \rho^2(\mathbf{r}) \rangle = \rho_{\text{smooth}}^2(\mathbf{r}) + \langle \rho_{\text{sub}}^2(\mathbf{r}) \rangle, \quad (5)$$

where $\langle \rho_{\text{sub}}^2(\mathbf{r}) \rangle$ means the average density square of subhalos according to the distribution probability. Since there is no correlation between the mass and spatial distribution in Eq. (4) we get $\langle \rho_{\text{sub}}^2(\mathbf{r}) \rangle$ at the position \mathbf{r} is given by an integral of mass

$$\begin{aligned} \langle \rho_{\text{sub}}^2(\mathbf{r}) \rangle &= \int_{m_{\text{min}}}^{m_{\text{max}}} n(m_{\text{sub}}, r) \left(\int \rho_{\text{sub}}^2 dV \right) \cdot dm_{\text{sub}} \\ &= \frac{n_0}{1 + (r/r_H)^2} \int_{m_{\text{min}}}^{m_{\text{max}}} f(m_{\text{sub}}) \cdot dm_{\text{sub}}, \end{aligned} \quad (6)$$

where ρ_{sub} refers to density of the subhalo at \mathbf{r} and V is its volume. We defined a function $f(m_{\text{sub}})$ in the equation above as

$$f(m_{\text{sub}}) = \left(\frac{m_{\text{sub}}}{M_{\text{vir}}} \right)^{-1.9} \int 4\pi r'^2 \rho_{\text{sub}}^2(r') dr', \quad (7)$$

which depends only on the subhalo mass since the virial radius and the density profile are all determined by the subhalo mass. The minimal subhalos is taken as $10^{-6} M_{\odot}$ [25] while the maximal mass of substructures is taken to be $0.01 M_{\odot}$ [46].

We notice that there are unphysical singularities at the center of the subhalo which may lead to $f(m_{\text{sub}})$ divergent. A cutoff r_{cut} is introduced within which the DM density is kept constant due to the balance between the annihilation rate and the rate to fill the region by infalling DM particles [47]. The time scale of the free fall of the DM particles can be approximately given by [47]

$$\tau \sim \frac{1}{\sqrt{G\bar{\rho}}}, \quad (8)$$

while the annihilation time scale is

$$\tau \sim \frac{1}{\langle \sigma v \rangle n_{\chi}(r_{\text{cut}})}. \quad (9)$$

Taking $\bar{\rho}$ about 200 times the critical density and $\langle \sigma v \rangle \sim 10^{-26} \text{ cm}^3 \text{s}^{-1}$ and applying the formulas above we then get $\rho_{\text{max}} \sim 10^{18} - 10^{19} M_{\odot}/\text{kpc}^3$, which corresponds to $r_{\text{cut}} \sim 10^{-8} - 10^{-7}$ kpc for the $\gamma = 1.7$ profile, $10^{-9} - 10^{-8}$ kpc for the Moore profile and can reach 10^{-11} kpc for NFW profile. In the following discussion, $\rho_{\text{max}} = 10^{18} M_{\odot}/\text{kpc}^3$ is adopted for NFW and Moore profiles while we consider $\rho_{\text{max}} = 10^{18} - 2 \times 10^{19} M_{\odot}/\text{kpc}^3$ for the profile with $\gamma = 1.7$. The results for NFW and Moore profile are not sensitive to r_{cut} [46], while for the profile with $\gamma = 1.7$ the result will change about 2 times.

The quantity $m_{\text{sub}} \times f(m_{\text{sub}})$ is plotted in Fig. 1. The figure shows the relative importance of different mass subhalos contributing to the annihilation signals. We can see from this figure that extending the minimal subhalo mass from the present numerical resolution of about $10^6 M_{\odot}$ to $10^{-6} M_{\odot}$ improves the contribution ~ 4 times larger.

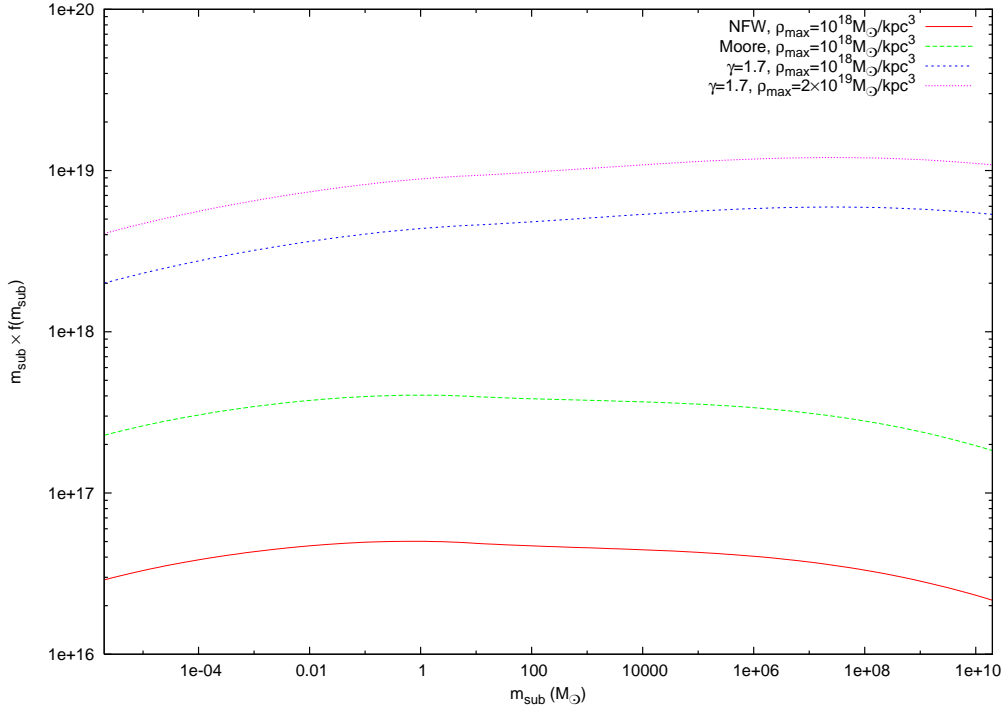


Figure 1. $m_{\text{sub}} \times f(m_{\text{sub}})$ as a function of subhalo mass m_{sub} .

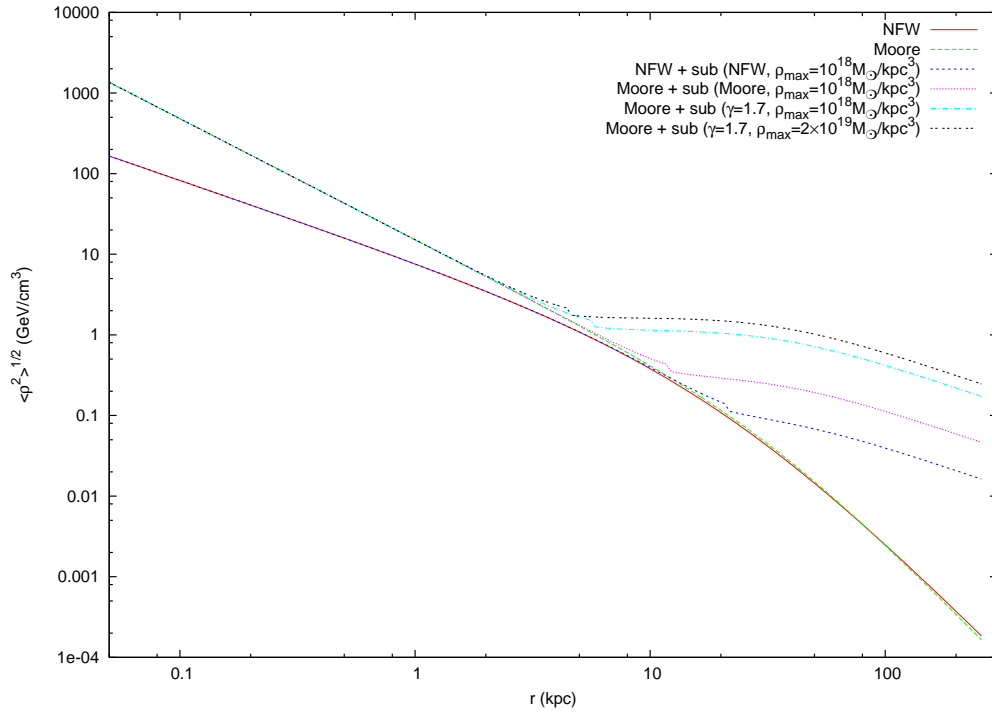


Figure 2. $\langle \rho^2(r) \rangle^{1/2}$ distribution for various DM profiles.

Fig. 2 shows $\langle \rho^2 \rangle^{1/2}$ for different DM profiles. We can see from this figure that the existence of subhalos will increase $\langle \rho^2 \rangle^{1/2}$ near the solar location, which will enhance the positron flux observed on the Earth.

4. The Positron Propagation

A complexity in calculating the positron flux is that positrons are scattered by the Galactic magnetic field (GMF) and we have to calculate its propagation in GMF. The propagation of charged particles in the GMF is diffusive. In addition they will also experience energy loss processes due to ionization and Coulomb interaction in the interstellar medium; for electrons and positrons there are additional synchrotron radiation in the GMF, bremsstrahlung radiation in the interstellar medium and inverse Compton scattering in the interstellar radiation field. The interaction between cosmic-ray particles and the interstellar medium (mostly Hydrogen and Helium) will lead to the fragmentation of nuclei. For radioactive nuclei the decay should also be taken into account.

The full propagation equation including the convection of cosmic-ray particles and reacceleration processes is written in the form

$$\begin{aligned} \frac{\partial \psi}{\partial t} = Q(\mathbf{x}, p) + \nabla \cdot (D_{xx} \nabla \psi - \mathbf{V} \psi) + \frac{\partial}{\partial p} p^2 D_{pp} \frac{\partial}{\partial p} \frac{1}{p^2} \psi \\ - \frac{\partial}{\partial p} \left[\dot{p} \psi - \frac{p}{3} (\nabla \cdot \mathbf{V} \psi) \right] - \frac{\psi}{\tau_f} - \frac{\psi}{\tau_r}, \end{aligned} \quad (10)$$

where ψ is the density of cosmic ray particles per unit momentum interval, $Q(\mathbf{x}, p)$ is the source term, D_{xx} is the spatial diffusion coefficient, \mathbf{V} is the convection velocity. The third term describes the reacceleration using diffusion in momentum space. \dot{p} is the momentum loss rate, τ_f and τ_r are timescales for fragmentation and radioactive decay respectively.

The interaction between cosmic-ray particles and the interstellar medium produces the secondary particles, such as positrons, antiprotons and some other heavy elements. The source term of the secondary cosmic-rays is given by

$$Q(\mathbf{x}, p) = \beta c \psi_p(\mathbf{x}, p) [\sigma_H(p) n_H(\mathbf{x}) + \sigma_{He}(p) n_{He}(\mathbf{x})], \quad (11)$$

where $\psi_p(\mathbf{x}, p)$ is the density of primary cosmic-rays, βc is the velocity of particles, σ_H and σ_{He} are the production cross sections for the secondary particles from the progenitor on H and He targets, n_H and n_{He} are the interstellar Hydrogen and Helium number densities, respectively.

The propagation equation (10) can be solved analytically under some simplification assumptions [18, 48]. A numerical solution to Eq. (10) is given in the GALPROP model developed by Strong and Moskalenko [28], which takes all the relevant processes into account. The realistic distributions for the interstellar gas and radiation fields are adopted in GALPROP. The detailed description of this model can be found in [28].

The secondary-primary ratio such as B/C depends on the propagation processes sensitively. The propagation parameters are adjusted to satisfy the B/C ratio, the electron and proton spectra *et al*. We include the nuclei up to $Z = 28$ and relevant isotopes. The injection spectra of protons and heavier nuclei are assumed to have the same power-law form in rigidity. The nuclei injection index below and above the

reference rigidity at 9 GV are taken as 1.98 and 2.42 respectively. The electron injection index below and above 4 GV are taken as 1.60 and 2.54 respectively. For propagation, we use the diffusion reacceleration model [49]. The spatial diffusion coefficient is taken as $\beta D_0(\rho/\rho_0)^\delta$, where $D_0 = 5.4 \times 10^{28} \text{ cm s}^{-1}$, $\rho_0 = 4 \text{ GV}$, and $\delta = 0.33$. The Alfvén speed is $v_A = 30 \text{ km s}^{-1}$. The height of the propagation halo is taken as $z_h = 4 \text{ kpc}$.

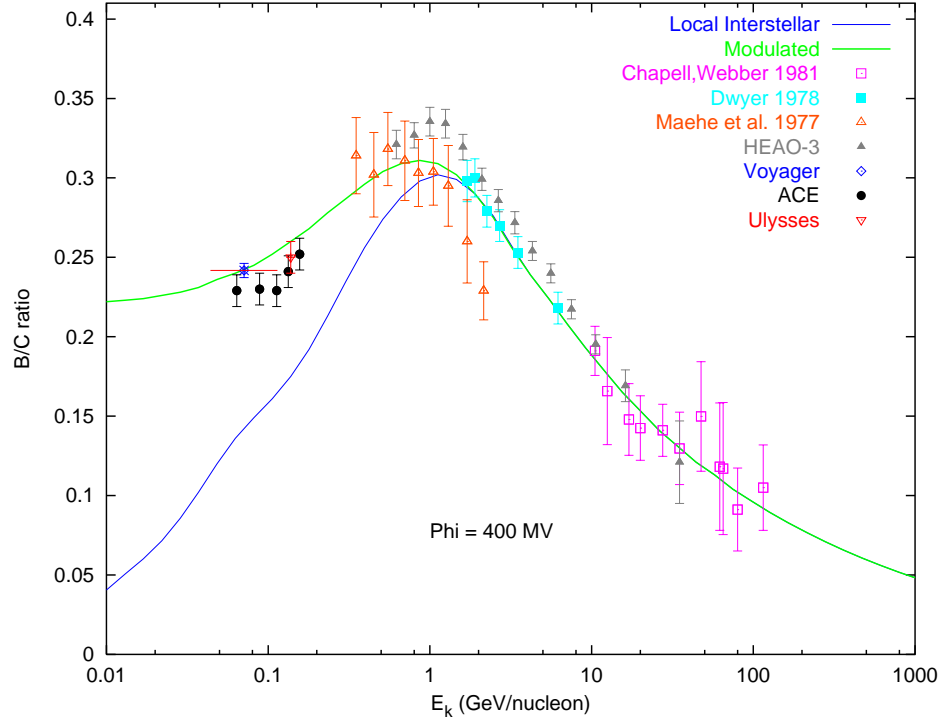


Figure 3. Calculated Boron-to-Carbon ratio compared with observational data. The lower line represents the local interstellar value, while the upper one is the result after solar modulation with $\Phi = 400 \text{ MV}$. Observational data: ACE [50], Ulysses [51], Voyager [52], HEAO-3 [53], for others please refer to [54].

In Figs. 3 and 4 we show B/C, the electron and proton spectra respectively. The propagation model describes the observational data very well. We will use this model to calculate the secondary positron spectrum from cosmic rays fragmentation given in Eq. (11) and the primary positron propagation from DMA given in Eq. (1).

5. Results and Discussion

Once the SUSY model is specified and the contribution from subhalos are taken into account we can incorporate the source term of primary positrons in GALPROP and calculate its spectrum on the Earth. In Fig. 5 we show the positron fluxes for three different SUSY models with $m_\chi = 121, 195, 242 \text{ GeV}$. The spectra are somewhat different for the three models because these models lead to different annihilation final states. All these models can help to account for the positron excess observed in HEAT. When

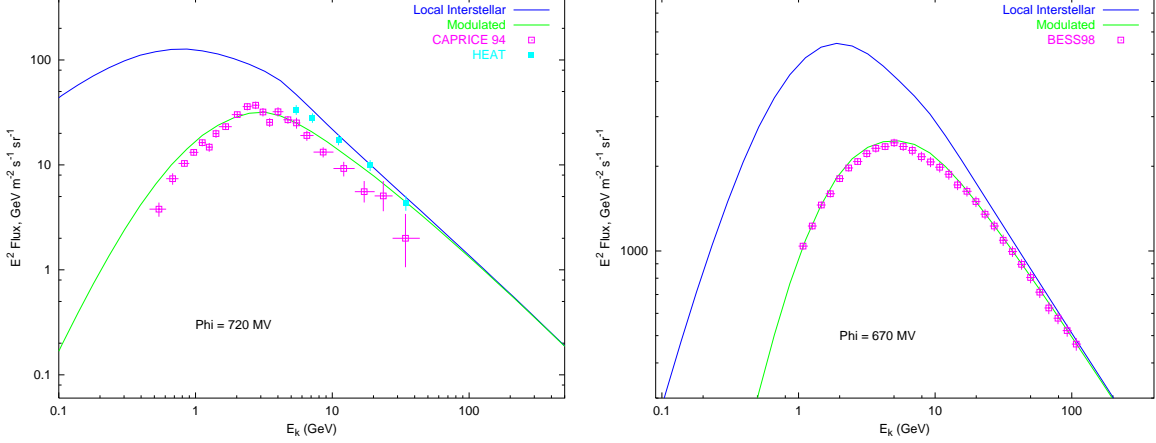


Figure 4. Electron and proton spectra for the same propagation model as B/C. The upper curve of each panel is the local interstellar result and the lower one is that after the solar modulation. Electron data: CAPRICE 94 [55], HEAT [56]; proton data: BESS 98 [57]

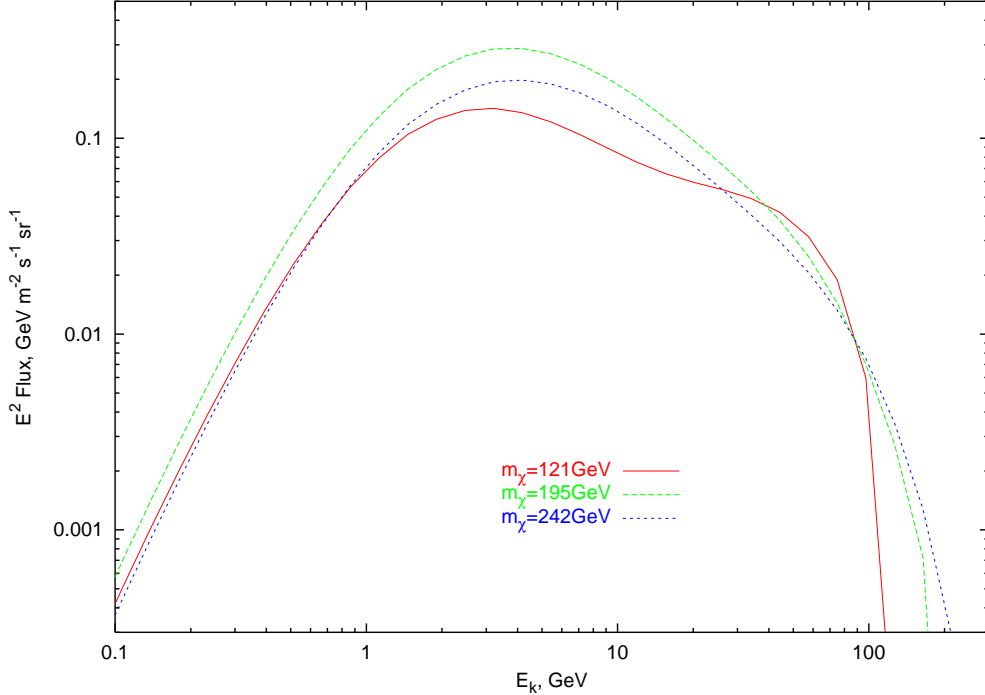


Figure 5. Positron flux on Earth for various neutralino mass. Moore profile, containing subhalos with $\gamma = 1.7$ and $\rho_{\max} = 2 \times 10^{19} M_{\odot}/kpc^3$ is adopted.

calculating the spectra, a Moore profile for the smooth component and $\gamma = 1.7$ profile for subhalos with $\rho_{\max} = 2 \times 10^{19} M_{\odot}/kpc^3$ are adopted.

In Fig. 6 we show the positron flux from the $m_{\chi} = 121 GeV$ model for different DM profiles. It indicates that the fluxes have several times differences among various DM profiles. The cuspier profiles lead to higher positron fluxes. It should be noted that

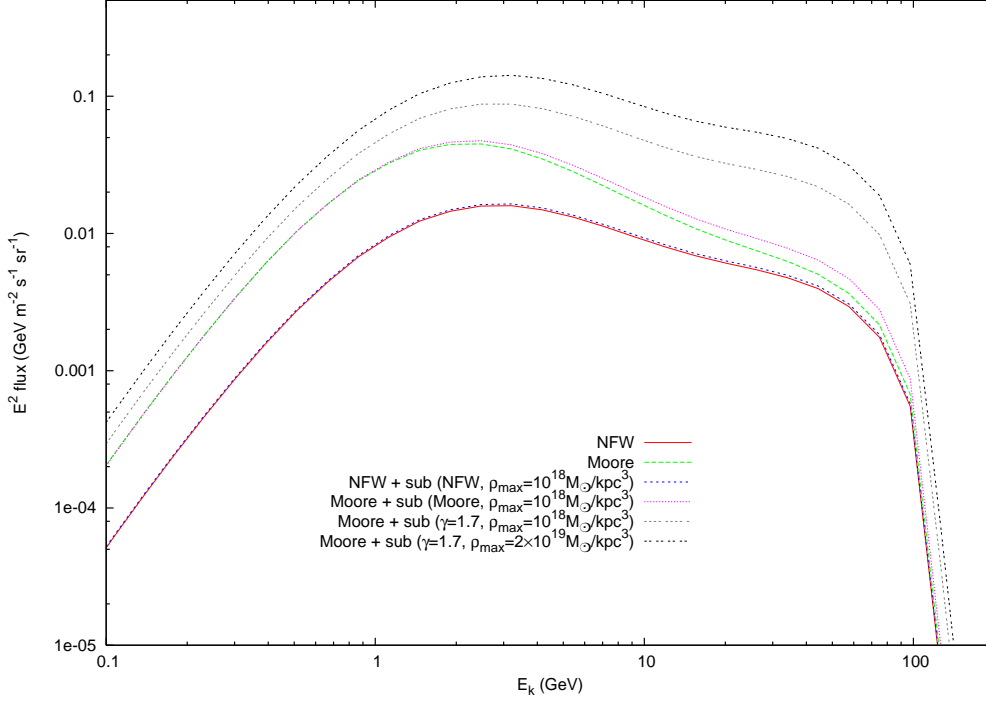


Figure 6. Positron flux on Earth for various DM profiles. The mass of neutralino is 121GeV .

because of the propagation effects the spectra from different DM profiles are different, although they have the same source spectrum. At lower energy the fluxes have bigger differences, since the low energy positrons have longer propagation distance, and may trace the $\langle \rho^2 \rangle$ farther away from the Earth. The differences between the NFW (or Moore) profile with and without subhalos are not significant. For subhalos with $\gamma = 1.7$ profile the flux is greatly enhanced.

We then compared the results between GALPROP and other propagation methods. The results are shown in Fig. 7. The fluxes for $m_\chi = 121$ and 242 GeV based on the Green's functions given by Kamionkowski & Turner [58], Baltz & Edsjo [18] and Moskalenko & Strong [59] are plotted. Specifically the Green's functions in [59] are given by fitting the GALPROP results. The similarity between our result and their result above 1 GeV confirms our calculation in GALPROP. The figure shows a remarkable discrepancy between the different models, especially at low-energy band. The reason of this inconsistency might come from some simplifications when finding the analytical Green's functions. The ignored effects might play an important role in the propagation. At low energies the discrepancy is large because of longer propagation path. GALPROP adopts realistic astrophysical inputs and may give more precise descriptions of the propagation than the Green's function method.

To give a consistent Galactic positron flux we calculate the background (secondary) positron fraction generated by interaction between primary cosmic-rays and interstellar gas in the same propagation model using GALPROP. In the Figs. 8, 9 we give

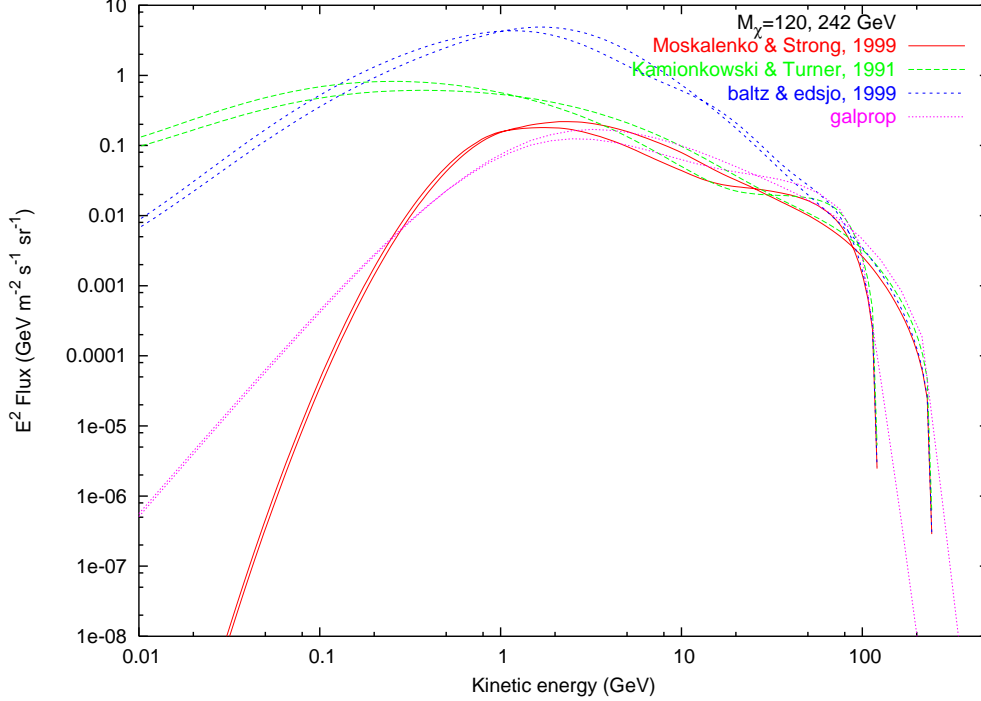


Figure 7. Comparison of positron fluxes of different propagation models.

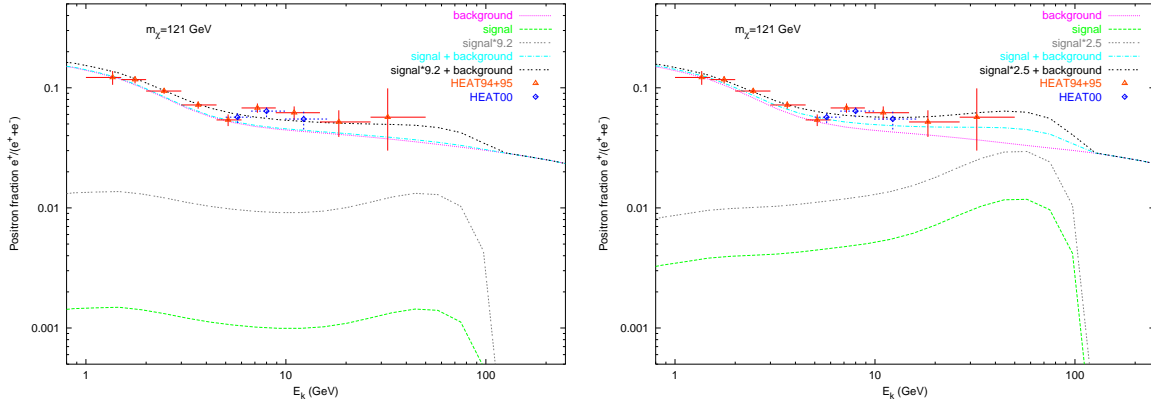


Figure 8. Positron fraction $e^+/(e^+ + e^-)$ calculated in this work. The left panel shows the result of a Moore DM profile, $\rho_{\max} = 10^{18} M_{\odot}/kpc^3$, without substructures. The right one is the same as the left but including the subhalos with $\gamma = 1.7$ and $\rho_{\max} = 2 \times 10^{19} M_{\odot}/kpc^3$. Data points are HEAT measurements in the three flights in 1994, 1995 and 2000 [20, 21].

the background positron fraction. Our results give better description to HEAT data compared with the adopted background fraction in [18, 19, 23, 26]. Therefore the new result requires a smaller “boost factor” to the DMA signals.

Adding the positron flux coming from DM annihilation to the secondary positrons, we get the total positron flux. The positron fraction $e^+/(e^+ + e^-)$ is plotted in Fig. 8 for $m_{\chi} = 121$ GeV. We can see from this figure that the expectation reproduces the measurements relatively well if DM subhalos are taken into account. The model with

subhalos can contribute several times more than that without subhalos. The best fit to the HEAT data requires “boost factors” of 9.2 and 2.5 for signals from DMA without and with subhalos respectively.

We do not think the discrepancy of a factor 2.5 is serious since there are large uncertainties in calculating the positron fluxes. Firstly there are large uncertainties for the positron propagation, as shown in Fig. 7. Secondly the random distribution of DM subhalos may have large variance as discussed in [27] since positrons lose energy quickly and have large fluctuations. The variance may lead to large positron flux due to accident, while in this work we just give the average positron flux. Thirdly we can choose SUSY model which produces more positrons, as shown in Fig. 9 for a model with $m_\chi = 195\text{GeV}$. The best fit to HEAT data requires a factor of 1.2 for this model. We should note that here we assume the thermal production of DM particle without introducing the nonthermal production as done in [19].

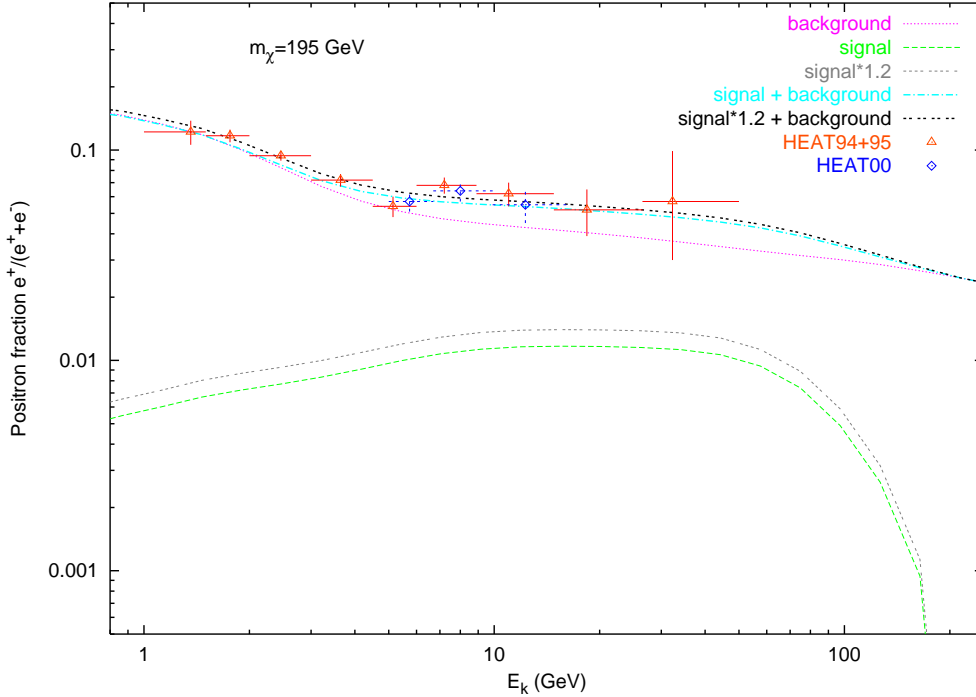


Figure 9. The same as Fig. 8 but for neutralino with mass $m_\chi = 195\text{GeV}$.

It is interesting to notice that at about 8GeV , HEAT measurements show some fine structures of the positron fraction, which does not appear in the neutralino annihilation spectrum. Maybe there are some specific sources or some specific physical process to generate positrons at this energy. However, the errors of the data are too big to give a definite assertion of this property. If it is confirmed by further experiments such as AMS-2, there should be deeper studies about the models we used here.

In summary, in this work we give a consistent and detailed calculation of the Galactic positron flux. We recalculate the background positron flux from cosmic ray collisions with the interstellar gas in a realistic propagation model GALPROP. The

results soft the discrepancy between data and expectations. For the primary positrons from DM annihilation we take the enhancement of subhalos into account. The result shows that the HEAT data can be explained by the two components without introducing “boost factor” or nonthermal production of DM. To account for the excess of positron flux extending subhalo masses to $10^{-6} M_{\odot}$ and requiring a cuspy profile as $\gamma = 1.7$ are necessary.

Acknowledgments

We thank Igor V. Moskalenko for great help on using the package GALPROP. This work is supported in part by the NSF of China under the grant No. 10575111, 10105004, 10120130794 and supported in part by the Chines Academy of Sciences.

Reference

- [1] Jungman G, Kamionkowski M and Griest K, *Supersymmetric dark matter*, 1996, *Phys. Rept.* **267** 195
- [2] Begeman K G, Broeils A H and Sanders R H, *Extended rotation curves of spiral galaxies - dark haloes and modified dynamics*, 1991, *Mon. Not. R. Astron. Soc.* **249** 523
- [3] Tyson J A and Fischer P, *Measurement of the mass profile of Abell 1689*, 1995, *Astrophys. J.* **446** 55
- [4] White S D M, Navarro J F, Evrard A E and Frenk C S, *The baryon content of Galaxy clusters - a challenge to cosmological orthodoxy*, 1993, *Nature* **366** 429
- [5] Peebles P J E, 1971, *Physical Cosmology* (Princeton: Princeton University Press)
- [6] Davis M, Efstathiou G, Frenk C S and White S D M, *The evolution of large-scale structure in a universe dominated by cold dark matter*, 1985, *Astrophys. J.* **292** 371
- [7] Spergel D N, Verde L, Peiris H V et al , *First-year Wilkinson Microwave Anisotropy Probe (WMAP) observations: determination of cosmological parameters*, 2003, *Astrophys. J. Supp.* **148** 175; Spergel D N et al , *Wilkinson Microwave Anisotropy Prob(WMAP) three year results: implications for comology*, 2006, *Preprint astro-ph/0603449*
- [8] Bertone G, Hooper D and Silk J, *Particle dark matter: evidence, candidates and constraints*, 2004, *Phys. Rept.* **405** 279
- [9] Goodman M W and Witten E, *Detectability of certain dark-matter candidates*, 1985, *Phys. Rev. D.* **31** 3059
- [10] Bottino A, de Alfaro V, Fornengo N et al , *On the neutralino as dark matter candidate. II. Direct detection* 1994, *Astropart. Phys.* **2** 77
- [11] Bernabei R, Belli P, Montecchia F et al , *Searching for WIMPs by the annual modulation signature*, 1998, *Phys. Lett. B.* **424** 195
- [12] Bernabei R, Belli P, Montecchia F et al , *On a further search for a yearly modulation of the rate in particle Dark Matter direct search*, 1999, *Phys. Lett. B.* **450** 448
- [13] Munoz C, *Dark matter detection in the light of recent experimental results*, 2004, *Int. J. Mod. Phys. A* **19** 3093
- [14] Barger V D, Halzen F, Hooper D et al , *Indirect search for neutralino dark matter with high energy neutrinos*, 2002, *Phys. Rev. D.* **65** 075022
- [15] Bergstrom L, Edsjo J and Ullio P, *Spectral gamma-ray signatures of cosmological dark matter annihilations*, 2001, *Phys. Rev. Lett.* **87** 251301
- [16] de Boer W, Herold M, Sander C et al , *Excess of EGRET Galactic gamma ray data interpreted as dark matter annihilation*, 2004, *Preprint astro-ph/0408272*

- [17] Donato F, Fornengo N, Maurin D *et al* , *Antiprotons in cosmic rays from neutralino annihilation*, 2004, *Phys. Rev. D* **69** 063501
- [18] Baltz E A and Edsjo J, *Positron propagation and fluxes from neutralino annihilation in the halo*, 1999, *Phys. Rev. D* **59** 023511
- [19] Kane G L, Wang L T and Wang T T, *Supersymmetry and the cosmic ray positron excess*, 2002, *Phys. Lett. B* **536** 263; Kane G L, Wang L T and Wells J D, *Supersymmetry and the positron excess in cosmic rays*, 2002, *Phys. Rev. D* **65** 057701
- [20] Barwick S W, Beatty J J, Bhattacharyya A *et al* , *Measurements of the cosmic-ray positron fraction from 1 to 50 GeV*, 1997, *Astrophys. J.* **482** L191
- [21] Couto S, Beach A S, Beatty J J *et al* , *Positron measurements with the Heat-pbar instrument*, 2001, *International Cosmic Ray Conference* 1687
- [22] Moskalenko I V and Strong A W, *Production and propagation of cosmic-ray positrons and electrons*, 1998, *Astrophys. J.* **493** 694
- [23] Baltz E A, Edsjo J, Freese K *et al* , *Cosmic ray positron excess and neutralino dark matter*, 2002, *Phys. Rev. D* **65** 063511
- [24] Hooper D, Taylor J E and Silk J, *Can supersymmetry naturally explain the positron excess?* 2004, *Phys. Rev. D* **69** 103509
- [25] Diemand J, Moore B and Stadel J, *Earth-mass dark-matter haloes as the first structures in the early Universe*, 2005, *Nature* **433** 389
- [26] Cumberbatch D T, Silk J, *Local dark matter clumps and the positron excess*, 2006, astro-ph/0602320.
- [27] Lavalle J, Pochon J, Salati P and Taillet R, *Clumpiness of dark matter and positron annihilation signal: computing the odds of the Galactic lottery*, 2006, Preprint astro-ph/0603796
- [28] Strong A W and Moskalenko I V, *Propagation of Cosmic-Ray Nucleons in the Galaxy*, 1998, *Astrophys. J.* **509** 212
- [29] Gondolo P, Edsjo J, Bergstrom L *et al* , *DarkSUSY - A numerical package for dark matter calculations in the MSSM*, 2000, Preprint astro-ph/0012234
- [30] Zhao H S, *Analytical models for galactic nuclei*, 1996, *Mon. Not. R. Astron. Soc.* **278** 488
- [31] Navarro J F, Frenk C S and White S D M, *A universal density profile from hierarchical clustering*, 1997, *Astrophys. J.* **490** 493
- [32] Moore B, Governato F, Quinn T *et al* , *Resolving the structure of cold dark matter halos*, 1998, *Astrophys. J.* **499** L5
- [33] Jing Y P and Suto Y, *The density profiles of the dark matter halo are not universal*, 2000, *Astrophys. J.* **529** L69; Jing Y P and Suto Y, *Triaxial modeling of halo density profiles with high-resolution N-body simulations*, *Astrophys. J.* **574** 538
- [34] Reed D, Governato F, Verde J *et al* , *Evolution of the density profiles of dark matter haloes*, 2005, *Mon. Not. R. Astron. Soc.* **357** 82
- [35] Bullock J S, Kolatt T S, Sigad Y *et al* , *Profiles of dark haloes: evolution, scatter and environment*, 2001, *Mon. Not. R. Astron. Soc.* **321** 559
- [36] Tormen G, Diaferio A & Syer D, *Survival of substructure within dark matter haloes*, 1998, *Mon. Not. R. Astron. Soc.* **299** 728
- [37] Klypin A, Gottlöber S, Kravtsov A V and Khokhlov A M, *Galaxies in N-body simulations: overcoming the overmerging problem*, 1999, *Astrophys. J.* **516** 530; Klypin A *et al* , *Where are the missing galactic satellites?* 1999, *Astrophys. J.* **522** 82
- [38] Moore B, Ghigna S, Governato F *et al* , *Dark matter substructure within Galactic halos*, 1999, *Astrophys. J.* **524** L19
- [39] Ghigna S, Moore B, Governato F *et al* , *Density profiles and substructures of dark matter halos: converging results at ultra-high numerical resolution*, 2000, *Astrophys. J.* **544** 616
- [40] Springel V, White S D M, Tormen G and Kauffmann G, *Populating a cluster of galaxies - I. results at z = 0*, 2001, *Mon. Not. R. Astron. Soc.* **328** 726
- [41] Zentner A R and Bullock J S, *Halo substructure and the power spectrum*, 2003, *Astrophys. J.* **598**

49

- [42] De Lucia G, Kauffmann G, Springel V *et al* , *Substructures in cold dark matter haloes*, 2004, *Mon. Not. R. Astron. Soc.* **348** 333
- [43] Kravtsov A V, Gnedin O Y and Klypin A A, *The tumultuous lives of galactic dwarfs and the missing satellites problem*, 2004, *Astrophys. J.* **609** 482
- [44] Diemand J, Moore B and Stadel J, *Velocity and spatial biases in cold dark matter subhalo distributions*, 2004, *Mon. Not. R. Astron. Soc.* **352** 535
- [45] Gao L, White S D M, Jenkins A, Stoehr F and Springel V, *The subhalo populations of Λ CDM dark haloes*, 2004, *Mon. Not. R. Astron. Soc.* **255** 819
- [46] Bi X J, *Gamma rays from the neutralino dark matter annihilations in the Milky Way substructures*, 2006, *Nucl. Phys. B.* **741** 83; Bi X J, Guo Y Q, Hu H B and Zhang X, *Detecting the dark matter annihilation at the ground EAS detectors*, 2006, *Preprint hep-ph/0610387*
- [47] Berezhinsky V S, Gurevich A V and Zybin K P, *Distribution of dark matter in the galaxy and the lower limits for the masses of supersymmetric particles*, 1992, *Phys. Lett. B.* **294** 221
- [48] Mautin D, Donato F, Tailley R and Salati P, *Cosmic rays below $Z = 30$ in a diffusion model: new constraints on propagation parameters*, 2001, *Astrophys. J.* **555** 585
- [49] Moskalenko I V, Strong A W, Ormes J F and Potgieter M S, *Secondary antiprotons and propagation of cosmic rays in the Galaxy and heliosphere*, 2002, *Astrophys. J.* **565** 280
- [50] Davis A J *et al* , *On the low energy decrease in Galactic cosmic ray secondary/primary ratios*, 2000, in *AIP Conf. Proc.* **528** 421
- [51] DuVernois M A, Simpson J A and Thayer M R, *Interstellar propagation of cosmic rays: analysis of the ULYSSES primary and secondary elemental abundances*, 1996, *Å* **316** 555
- [52] Lukasiak A, *Voyager measurements of the charge and isotopic composition of cosmic ray Li, Be and B nuclei and implications for their production in the Galaxy*, 1999, *Proc. 26th Int. Cosmic Ray Conf.* **3** 41
- [53] Engelmann J J, Ferrando P, Soutoul A, Goret P and Juliusson E, *Charge composition and energy spectra of cosmic-ray nuclei for elements from Be to Ni - results from HEAO-3-C2*, 1990, *Å* **233** 96
- [54] Stephens S A and Streitmatter R E, *Cosmic-ray propagation in the Galaxy: techniques and the mean matter traversal*, 1998, *Astrophys. J.* **505** 266
- [55] Boezio M *et al* , *The cosmic-ray proton and Helium spectra between 0.4 and 200 GV*, 1999, *Astrophys. J.* **518** 457
- [56] DuVernois M A *et al* , *Cosmic-ray electrons and positrons from 1 to 100 GeV: measurements with HEAT and their interpretation*, 2001, *Astrophys. J.* **559** 296
- [57] Sanuki T *et al* , *Precise measurement of cosmic-ray proton and Helium spectra with the BESS spectrometer*, 2000, *Astrophys. J.* **545** 1135
- [58] Kamionkowski M and Turner M S, *Distinctive positron feature from particle dark-matter annihilations in the galactic halo*, 1991, *Phys. Rev. D.* **43** 1774
- [59] Moskalenko I V and Strong A W, *Positrons from particle dark-matter annihilation in the Galactic halo: propagation Green's functions*, 1999, *Phys. Rev. D.* **60** 063003